A SECOND-ORDER MAGNETOCALORIC MODEL SUBSTANCE FOR STANDARDIZATION PURPOSES

DIDIER VUARNOZ[1], PETER W. EGOLF[1], SERGIO GAMA[2], ADELINO A. COELHO[3]

[1]University of Applied Sciences of Western Switzerland
Institute of Thermal Sciences and Engineering
CH-1401 Yverdon-les-Bains, Switzerland

[2]Universidade Federal de São Paulo
UNIFESP – Campus DIADEMA
São Paulo, Brazil

[3]Universidade Estadual de Campinas
Unicamp, 13083-970 Campinas
São Paulo, Brazil

Peter.egolf@heig-vd.ch

ABSTRACT

Magneto **C**aloric **M**aterials (MCM's) are the working fluids (refrigerants) of magnetic heating/heat pumping, cooling/refrigeration and energy conversion. Physically they exhibit the magnetocaloric effect. The technologies applying these materials are coming increasingly into the focus of interest, and first approaches of magnetic refrigerators, e.g. wine coolers, etc., to refrigeration markets have been recently announced. – The physical modeling of devices operating with the **M**agneto **C**aloric **E**ffect (MCE) is often very cumbersome, because the experimental material data sets are incomplete or slightly erroneous, so that the obtained numerical results do not even fulfill energy conservation laws. In this article a phenomenological approach of modeling second-order magnetocaloric material properties is proposed, which allows highest accuracy in numerous kinds of numerical simulation processes. The presented model substance is also ideal for standardization purposes of physical modeling and numerical simulations of the operation of magnetic heaters, refrigerators and energy conversion machines.

Keywords: magnetocaloric, entropy, second-order magnetic phase transition, standardization

1. INTRODUCTION

The occurrence of advanced magnetic technologies, covering a wide field of technical applications, are making magnetic materials in our society more and more omnipresent and omnipotent (Gutfleisch et al., 2011). Among them are the electrocaloric and magnetocaloric materials (see e.g. Kitanovski et al., 2015). In this article, we focus on the second class of materials that exhibit a temperature rise when pushed into a magnetic field or inversely a decrease when pulled out of a magnetic field region. This effect is called **M**agneto **C**aloric **E**ffect (MCE) and is described, for example, in the standard text book of Tischin and Spichkin

(2003). In their book numerous measurements of the magnetocaloric properties are presented, which, for example, are the magnetization, the (specific) entropy change, the adiabatic temperature change and the magnetic and thermal specific heat capacities.

There exists a large amount of literature on the building of prototypes applying the MCE. For scientists interested in this area the following publications are recommended (Yu et al., 2010, Kitanovski et al., 2015). Efforts for implementing the MCE into numerous types of machines, e.g. refrigerators, heat pumps, air-conditioners, energy conversion and harvesting devices, etc., at present is increasing all over the world (see Egolf et al., 2014).

The International Institute of Refrigeration IIR/IIF has a Working Party on Magnetic Refrigeration. Based on difficulties to compare experimental results of magnetocaloric materials of different origin (Which purity of the material was applied (Gschneidner, 1993)? Which size of grains are present (Zeng et al., 2011)? Which magnetic field was applied (Kitanovski and Egolf, 2006)? Were demagnetization effects taken into consideration (Morrish 2001)? Were dynamic effects considered (Tishin et al., 2007)? etc.) and to compare numerical modeling results of prototypes (Which material data sets were considered? Which types of energy losses were taken into the calculation process? How much were magnetic field configurations idealized? etc.) its former President initiated standardization work. In this context the proposing of a universal curve to characterize the magnetic entropy change of MCM by Franco (see Franco et al., 2006 and Franco et al., 2008) is mentioned. In machine building, Kitanovski et al., (2009) and Rowe (2009) worked on the performance metrics of prototypes. Classification schemes of machines have been worked out by Scarpa et al., (2012).

There's no way to measure directly the degree of disorder described by the entropy *S*. Molecular **M**ean **F**ield **T**heory (MFT) and the **H**eisenberg **M**odel (HM) are the two main quantum mechanical theories to theoretically determine the magnetic entropy. For our purpose also they are not fully satisfactory. The calculation of the magnetic entropy change in the MFT is not so straightforward because of the transcendental character of the Brioullin function (Tishin and Spichkin, 2003). In the Heisenberg model, the MCE peak is located above the Curie temperature of the MCM (Franco et al., 2008).

This article reports on a first attempt to elaborate on a phenomenological model substance with properties close to those of pure gadolinium (Gd). The substance yields a complete data set which strictly obeys magneto-thermomagnetic laws (see Kitanovski and Egolf, 2006) with any predefined, respectively demanded, precision. The hope is that this model substance will be generally established for calculations and comparisons of the operation, the efficiency, etc. of machines applying the MCE to operate their specific magneto-thermodynamic cycles.

2. MATHEMATICAL FORMULATION OF THE PHYSICAL PROPERTIES

For most common MCM's, the total specific entropy s is the sum of three partial contributions, namely the magnetic s_m, the electronic s_e, and the lattice specific entropy s_l

$$s(H_0,T) = s_m(H_0,T) + s_e(T) + s_l(T)\,, \tag{1}$$

A representation of Eq. 1 is shown in FIG. 2 (small inserted figure) for the special case of no external or applied magnetic field H_0=0.

A virtual MCM, representing a second-order magnetic material with idealized physical properties, is designed by taking an empirical Ansatz with an exponential function. The magnetization, M, (see also FIG. 1) is described as function of the magnetic field, H_0, and temperature T by

$$\mu_0 M(H_0,T) = \mu_0 A(T-T_0)(1-e^{-\frac{\mu_0 H_0}{B(T-T_0)}}) + C(T-T_0)\mu_0 H_0, \qquad (2)$$

where μ_0 denotes the magnetic permeability and A,B and C are linear fitting functions

$$\mathrm{X}(T) = \chi_1 T + \chi_2, \qquad \mathrm{X} \in \{A,B,C\}, \qquad \chi \in \{a,b,c\}, \qquad (3a\text{-}c)$$

where the numerical coefficients are listed in Table 1. A vanishing shift of temperature (T_0=0) corresponds to a model description of Gd with a Curie temperature being (approximately) 293 K. Therefore, for example, to adjust this model substance to a magnetic energy conversion application with a virtual material with physical properties of Gd, but with a Curie temperature of T_C=300°C, one needs to insert T_0=280.2 K. However, in the following sections, for simplicity, we set T_0=0.

Table 1. Coefficients of the three linear functions characterizing the magnetization of Gd.

a_1 ($Am^{-1}K^{-1}$)	a_2 (Am^{-1})	b_1 ($T\,K^{-1}$)	b_2 (T)	c_1 (K^{-1})	c_2 (-)
$-5.53*10^3$	$2{,}52*10^6$	0.06	-16.42	$-9{,}72*10^{-4}$	$3{,}48*10^{-1}$

In FIG. 1 the model curves are compared with up-to-present unpublished measurements of the magnetization of Gd. However, the same material has already been applied in a prototype of a magnetic refrigerator (see Coelho et al., 2009).

A Maxwell relation is (see e.g. Kitanovski and Egolf, 2006)

$$\left.\frac{\partial M}{\partial T}\right|_{H_0} = -\frac{1}{\mu_0}\left.\left(\frac{\partial s}{\partial H_0}\right)\right|_T = -\frac{1}{\mu_0}\left.\left(\frac{\partial s_m}{\partial H_0}\right)\right|_T, \qquad (4a,b)$$

where the second identity follows from Eq. (1).

The left-hand term in Eq. (4a) follows by taking the derivative of Eq. (2) with respect to temperature

$$\left.\frac{\partial M}{\partial T}\right|_{H_0} = a_1 + c_1\mu_0 H_0 - \left(a_1 + \frac{A(T)\;b_1\mu_0 H_0}{B(T)^2}\right) e^{-\frac{\mu_0 H_0}{B(T)}}. \qquad (5)$$

With Eq. (4b) and (5), it follows

$$\left(\frac{\partial s_m}{\partial H_0}\right)\Bigg|_T = -\mu_0\left[a_1 + c_1\mu_0 H_0 - \left(a_1 + \frac{A(T)\ b_1\mu_0 H_0}{B(T)^2}\right) e^{-\frac{\mu_0 H_0}{B(T)}}\right]. \tag{6}$$

To obtain the specific entropy Eq. (6) is now integrated

$$s_m(H_0,T) = -\mu_0 \int_0^{H_0}\left[a_1 + c_1\mu_0 H - \left(a_1 + \frac{A(T)\ b_1\mu_0 H}{B(T)^2}\right) e^{-\frac{\mu_0 H}{B(T)}}\right] dH + s_m(0,T)\,, \tag{7}$$

In a two-dimensional integration there is an integration "constant" that is a function that depends only on the second variable over which no integration takes place. In our case this is a function depending on temperature T, but not on the magnetic field H_0. By setting H_0=0 the integral vanishes and one sees that this temperature dependent function must be identical to the specific magnetic entropy at zero magnetic field $s_m(0,T)$.

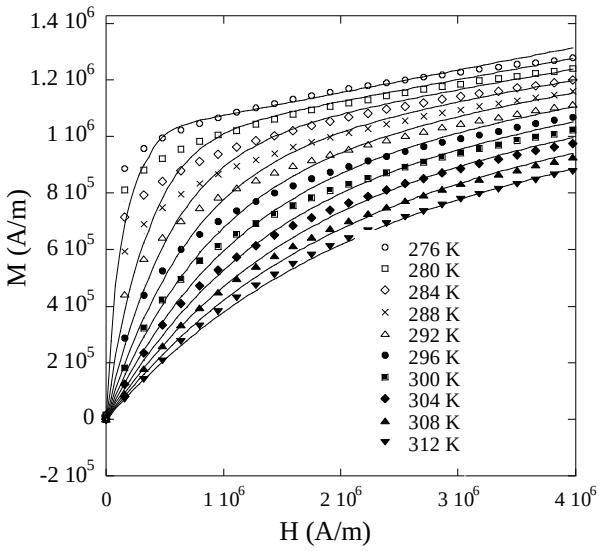

Fig. 1. The measured magnetization of Gd is shown by markers denoting different temperatures and the model curves by solid lines. The purity of this Gd, originating from China, is 99.9 %. It has been vacuum melted using a RF furnace. The magnetization was measured in a QDS (Quantum Design Squid).

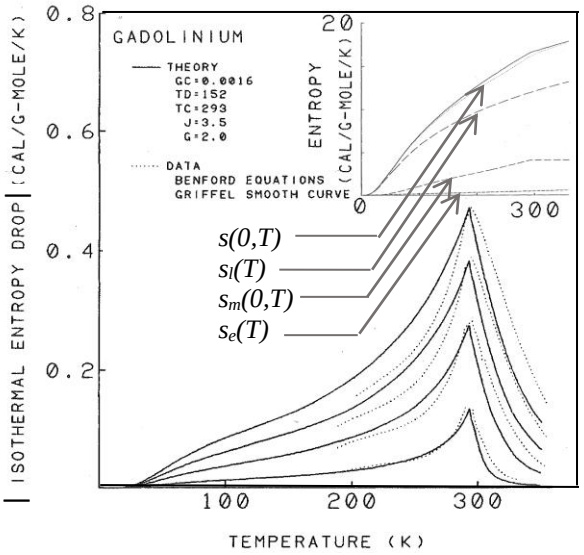

Fig. 2. Absolute value of the magnetic entropy change of Gd obtained with MFT (continuous lines) for the magnetic field strength H_0 = 1, 3, 5 and 7 T. The small inserted picture shows the specific entropy contributions for H_0 = 0 T (from Chen et al., 1991).

The temperature dependence of the magnetic entropy at zero magnetic field, $s_m(0,T)$, is taken from reference Chen et al. (1991) (see Fig. 2, inserted small picture). A linear fit of $s_m(0,T)$ is approximately given by the following empirical equation (SI units are applied)

$$s_m(0,T) = \begin{cases} 3699.9T - 216193, & \text{for } T < T_C \\ 8{,}7 * 10^5, & \text{for } T \geq T_C \end{cases} \tag{8}$$

The following integral formula is helpful to integrate the integral in Eq. (6)

$$\int x\ e^{-x}dx = -(1+x)e^{-x}, \qquad x = \frac{\mu_0 H}{B(T)}, \tag{9a,b}$$

where also a change of variable is applied. This leads to

$$s_m(H_0,T) = -\mu_0\left\{a_1 H_0 + \frac{c_1}{2}H_0^2 + \frac{a_1 B(T)}{\mu_0}\left(e^{-\frac{\mu_0 H_0}{B(T)}}\right) + \right.$$
$$\left.\frac{A(T)\ b_1}{\mu_0}\left[\left(1+\frac{\mu_0 H_0}{B(T)}\right)e^{-\frac{\mu_0 H_0}{B(T)}}\right] - \frac{a_1 B(T)}{\mu_0} - \frac{A(T)\ b_1}{\mu_0}\right\} + s_m(0,T). \tag{10}$$

From Eq. (1) and (10) the total specific entropy is derived

$$s(H_0,T) = -\mu_0\left\{a_1 H_0 + \frac{c_1}{2}H_0^2 + \frac{a_1 B(T)}{\mu_0}\left(e^{-\frac{\mu_0 H_0}{B(T)}}\right) + \frac{A(T)\ b_1}{\mu_0}\right.$$
$$\left.\left[\left(1+\frac{\mu_0 H_0}{B(T)}\right)e^{-\frac{\mu_0 H_0}{B(T)}}\right] - \frac{a_1 B(T)}{\mu_0} - \frac{A(T)\ b_1}{\mu_0}\right\} + s_m(0,T) + s_e(T) + s_l(T). \tag{11}$$

The first term on the right-hand side denotes the magnetic dependent part of the specific entropy. This is also identical to the specific magnetic entropy change

$$\Delta s_m(H_0,T) = s_m(H_0,T) - s_m(0,T) = -\mu_0\left\{a_1 H_0 + \frac{c_1}{2}H_0^2 + \frac{a_1 B(T)}{\mu_0}\left(e^{-\frac{\mu_0 H_0}{B(T)}}\right) + \right.$$
$$\left.\frac{A(T)\ b_1}{\mu_0}\left[\left(1+\frac{\mu_0 H_0}{B(T)}\right)e^{-\frac{\mu_0 H_0}{B(T)}}\right] - \frac{a_1 B(T)}{\mu_0} - \frac{A(T)\ b_1}{\mu_0}\right\}. \tag{12}$$

For a zero magnetic field, Eq. (11) simplifies to

$$s(0,T) = s_m(0,T) + s_e(T) + s_l(T)\,. \tag{13}$$

3. COHERENCE AND COMPATIBILITY TEST OF MEASUREMENTS

It makes sense to define the following quantity

$$s_m{}^*(H_0,T) = s_m(H_0,T) - \Delta s_m(H_0,T)\,. \tag{14}$$

From Eq. (10) and (12) it follows that this function does not depend on the magnetic field, because one concludes that

$$s_m{}^*(H_0,T) = s_m(0,T)\,. \tag{15}$$

This gives us the possibility to test if the measurements of the magnetization curves and the ones of the magnetic entropy change by Chen et al. (1991) correspond in the sense

that they do not violate the Maxwell relation. To do so, we take our magnetization curve fits to our data shown in FIG. 1. Then we calculate with Eq. (10) the integral part of $s_m(H_0,T)$ and add $s_m(0,T)$, determined by Chen et al. and shown in the inset of FIG. 2, to obtain $s_m(H_0,T)$. These results are shown for three magnetic fields, namely 1, 3 and 5 T in FIG. 3 by the curves with solid lines. By applying Eq. (14), we then determine (also for the three magnetic fields) $s_m^*(H_0,T)$. The three resulting curves were additively shifted to values corresponding to Chen et al.'s measurements to obey the condition $s_m(H_0,0)=0$. They are shown in FIG. 4. As predicted by the model (compare with Eq. (15)) these curves fall with good accuracy onto a single curve and by this demonstrate coherence and compatibility. This is a positive result confirming a very good quality of the measurements of the two research groups. Notice that the small deviations of the three curves in FIG. 4 have three origins:

1) Error in experimental determination of magnetization
2) Error in curve fitting of the magnetization curves
3) Error in experimental determination of the specific entropy.

It must be mentioned that there are measurements in the literature that do not show very good coherence and compatibility test results.

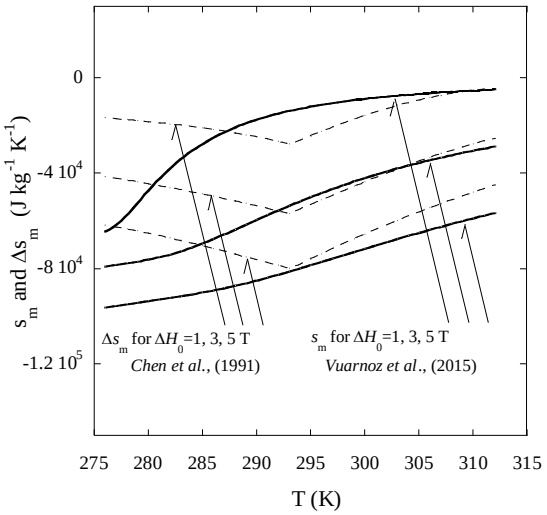

Fig. 3. The solid lines show the magnetic specific entropy determined by our model calculations (see Eq. (10) for magnetic field changes of 1, 3 and 5 T. The dotted lines show the three magnetic entropy changes (from Ref. Chen et al., 1991).

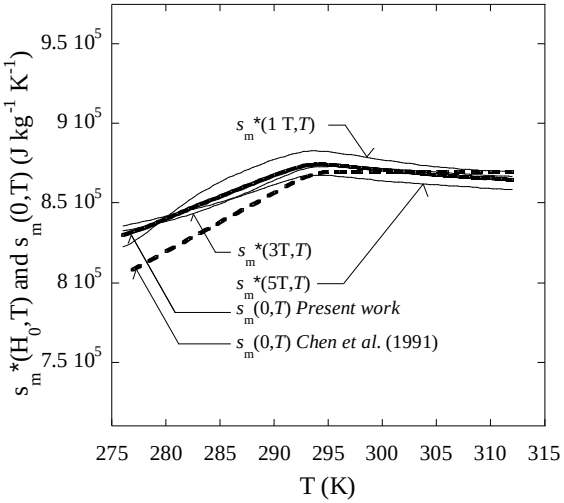

FIG. 4. The three functions $s_m^*(H_0,T)$ for the three magnetic field strength are presented. Their mean value is shown as $s_m(0,T)$ (present work). For comparison the same function, determined by Chen et al., (1991), is also shown.

We then determined the mean value of the three curves $s_m(H_0,T)$ (see Eq. (8)) and replaced in Eq.'s (10) and (11) Chen's $s_m(0,T)$ by this function. With this final result of our model, the curves $s(H_0,T)$ shown in FIG. 6 were determined with help of Eq. (11) to draw the thermodynamic T-s diagram. Furthermore, FIG. 5, which is the magnetic M-H_0 diagram, was determined by applying Eq. (2).

4. CYCLE ANALYSIS

The model is applied to draw the M-H_0 diagram and the T-s diagram. Into these diagrams an Ericsson cycle (see Kitanovski and Egolf, 2006), operating between the two magnetic fields of 0 and 2 T, has been drawn. The cold sink has a temperature of T_C=283 K and the hot source of T_H=303 K. Table 2 resumes the four corner points of the process.

Table 2. Physical properties of the MCM during a quasi-steady operation in a process named Ericsson cycle. The maximum magnetic field change is 2 T and the maximum temperature difference 20 °C. The area in the closed cycle corresponds to the performed work of a machine.

	T (K)	s_m (J m^{-3} K^{-1})	$\mu_0 H_0$ (T)	$\mu_0 M$ (T)
Pt 1	283	830.9 10^3	0	0
Pt 2	303	870.0 10^3	0	0
Pt 3	303	848.1 10^3	2	0.85
Pt 4	283	771.3 10^3	2	1.34

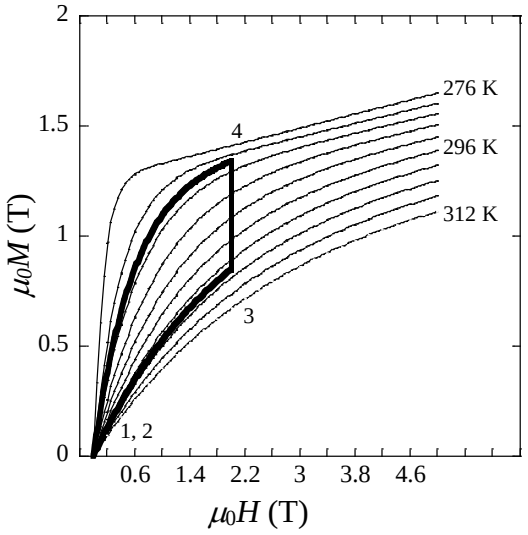

Fig. 5. A magnetic Ericsson cycle presented in a diagram of magnetism.

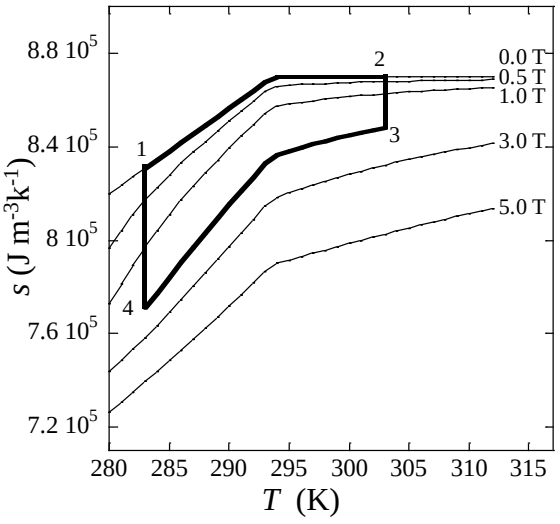

Fig. 6. The same magnetic Ericsson cycle presented in a diagram of thermodynamics.

By solving the circle integrals numerically for both cases, the results obtained are w = 7,5*10^5 J m^{-3} with a relative error between the two results of only 0.67 %. This demonstrates the high accuracy one can achieve by applying the proposed model substance to describe thermomagnetic processes.

5. CONCLUSIONS AND OUTLOOK

An “ideal” model substance which can be adjusted to describe the magneto-thermodynamic behavior of any magnetocaloric material, showing a *second-order phase transition*, is presented. In further work the specific heat and adiabatic temperature difference of this substance will be determined. Furthermore, the model shall be generalized to also describe the behavior of a MCM showing a *first-order phase transition*. In a succeeding work, for this a description similar to the presented model with limes solutions shall be derived and applied.

REFERENCES

Chen F.C., Murphy R.W., Mei V.C., Chen G.L., Lue J.W., Lubell M.S., 1991, *Loss analysis of the thermodynamic cycle of magnetic heat pumps*. ONRL/TM-11608, Oak Ridge, 83 p.

Coelho, A.A., Gama, S., Magnus, A., Carvalho, G., 2009, Prototype of a Gd-based rotating magnetic refrigerator for work around room temperature, *Third IIF-IIR International Conference on Magnetic Refrigeration at Room Temperature*, Des Moines, Iowa, USA, 11-13 May 11-15, 381-386.

Egolf P.W., Tishin A.M., Auracher H., 2014, New developments in magnetic refrigeration, *Special Issue Int. J. Refrigeration* 37: 1-318.

Franco V., Blázquez J. S., Conde A., 2006, Field dependence of the magnetocaloric effect in materials with a second order phase transition: A master curve for the magnetic entropy change. *Appl. Phys. Lett.* 89(22): 222512.

Franco V., Conde A., Romero-Enrique J.M., Blázquez J.S., 2008, A universal curve for the magnetocaloric effect: an analysis based on scaling relations. *J. Phys.: Cond. Matter*, 20(28): 285207.

Gutfleisch O., Willard M.A., Brück E., Chen C.H., Sankar S.G., Liu J.P., 2011, Magnetic materials and devices for the 21st century: stronger, lighter, and more energy efficient. *Adv. Mat.* 23(7): 821-842.

Gschneidner K.A., 1993, Metals, alloys and compounds-high purities do make a difference! *J. Alloys Comp.*, 193(1): 1-6.

Kitanovski A., Egolf P.W., 2006, Thermodynamics of magnetic refrigeration. *Int. J. Refrige*-tion 29: 3-21.

Kitanovski A., Gonin C., Vuarnoz D., Sari O., Egolf P.W. 2009, A standardization of the coefficient of performance for magnetic refrigerators, heat pumps and energy conversion machines. *Proc. Thermag III*, IIR/IIF: 229-237.

Kitanovski, A., Tušek, J., Tomc, U., Paznik, U., Ozbolt, M., Poredoš, A., 2015, *Magnetocaloric Energy Conversion*, Green Energy and Technologies, Springer Edition, Berlin, ISBN 978-3-319-08740-5.

Morrish, A., H., 2001, The Physical Principle of Magnetism, IEEE Press Classic Reissue, New York, ISBN 0-7803-6029-X.

Rowe A., 2009, Performance metrics for active magnetic refrigerators. *Third IIF-IIR International Conference on Magnetic Refrigeration at Room Temperature*, Des Moines, Iowa, 11-15 May, 195-205.

Scarpa F., Tagliafico G., Tagliafico L.A., 2012. Classification proposal for room temperature magnetic refrigerators. *Int. J. of Refrigeration* 35(2): 453-458.

Tishin, A.M., Spichkin, Y.I., 2003, *The Magnetocaloric Effect and its Applications*, Series of Condensed Matter Physics, Institute of Physics Publishing, Bristol, ISBN 0 7503-0922-9.

Tishin, A.M., Spichkin, Y.,I., Gschneidner, K.A., Jr., Pecharsky, V.K., 2007, Dynamic magnetocaloric effect, *Second IIF-IIR International Conference on Magnetic Refrigeration at Room Temperature*, Portorosz, Slovenia, 11-13 April, 35-45.

Yu B., Liu M., Egolf P.W., Kitanovski A., 2010, A review of magnetic refrigerator and heat pump prototypes built before the year 2010. *Int. J. of Refrig*eration 33 (6): 1029-1060.

Zeng H., Zhang J., Kuang C., Yue M., 2011, Magnetic entropy change in bulk nanocrystalline Gd metals. *Appl.Nano Sci.* 1(1): 51-57.